Draft version August 27, 2013
Preprint typeset using LaTeX style emulateapj v. 11/10/09

THE ORBITS OF THE TRIPLE STAR SYSTEM 1 GEMINORUM FROM *PHASES* DIFFERENTIAL ASTROMETRY AND SPECTROSCOPY

BENJAMIN F. LANE[1], MATTHEW W. MUTERSPAUGH[2,3], R. F. GRIFFIN[4], COLIN D. SCARFE[5,10], FRANCIS C. FEKEL[3,11], MICHAEL H. WILLIAMSON[3], JOEL A. EATON[3], SHRINIVAS R. KULKARNI[6], M. SHAO[7], M. M. COLAVITA[7], BERNARD F. BURKE[8], MACIEJ KONACKI[9]

Draft version August 27, 2013

ABSTRACT

We have used precise differential astrometry from the Palomar High-precision Astrometric Search for Exoplanet Systems (PHASES) project and radial-velocity measurements covering a time-span of 40 yrs to determine the orbital parameters of the 1 Geminorum triple system. We present the first detection of the spectral lines of the third component of the system, together with precise mass (0.5%) and distance (0.15%) determinations for this system. In addition, our astrometry allows us to make the first determination of the mutual inclination of the orbits.

Subject headings: techniques:interferometric–binaries:spectroscopic–stars:fundamental parameters–stars:individual (1 Gem)

1. INTRODUCTION

The star 1 Geminorum (HR 2134, HD 41116, HIP 28734, Kui 23AB) is a bright ($m_V = 4.15, m_K = 2.18$), nearby (∼47pc) triple system (Abt & Kallarakal 1963; Tokovinin 1997). Kuiper (1948) made the serendipitous discovery of the A–B close visual binary system, which has an apparent semi-major axis of $0\farcs20$ and an orbital period of 13.3 years. The A component is evolved and has a spectral type of K0 III (Abt & Kallarakal 1963), while the B component is a short-period binary system with a 9.60-day period(Griffin & Radford 1976). Strassmeier & Fekel (1990) determined the spectral type of the brighter component of the B system (which we will refer to as Ba) to be F6 IV. To our knowledge, no detections of the fainter component, Bb, have been published. Griffin & Radford (1976) and Griffin (1980) have provided the history of earlier work on this bright triple system.

Multiple stellar systems such as 1 Gem are of interest for several reasons. First, it is possible to measure masses of the individual components and the system distance directly with high precision, while the presence of several stars provides further constraints for stellar models by requiring the binary component stars to be co-eval (Torres & Ribas 2002). This is particularly important in a system such as 1 Gem, where one or more of the components has evolved off the main sequence. Second, as pointed out by Sterzik & Tokovinin (2002), the relative orientations of the orbital angular momenta allow one to constrain the properties of the cloud from which the stars are thought to have formed, as well as the subsequent dynamical decay process, or lack thereof (Tokovinin 2008). Finally, the dynamical interactions of the stars may provide interesting constraints on the magnitude of tidal interactions (Kiseleva et al. 1998; Kiseleva-Eggleton & Eggleton 2001). However, given the often wide range of orbital separations and periods, multiple stars are challenging observational targets that usually require observations by two techniques (imaging and spectroscopy), and so to date only a handful of such systems have been fully characterized (Eggleton & Tokovinin 2008).

Advances in long-baseline stellar interferometry now enable astrometry (Lane & Muterspaugh 2004) with 35 μ-second-of-arc precision and have made it possible to resolve the orbital motion of several interesting multiple systems (Muterspaugh et al. 2006a,b; Lane et al. 2007; Muterspaugh et al. 2008, 2010b). Here we continue this work with a report on astrometry of the 1 Gem system. For the first time we are able to determine the orbital inclination of the close binary system (Ba–Bb), as well as the mutual inclination of the two orbits.

However, astrometry alone is not sufficient to determine fully the orbital and stellar properties of this system. We also present the results of extensive radial-velocity campaigns at various observatories that have followed this system for up to nearly three complete orbital periods of the visual binary. With the combination of our data, which includes 29 PHASES astrometric measurements and 1799 radial velocities, plus 63 high-angular-resolution observations from the literature, we are able to

[1] The Charles Stark Draper Laboratory, Inc., 555 Technology Sq., Cambridge MA 02139 USA
[2] Department of Mathematical Sciences, College of Engineering, Tennessee State University, Boswell Science Hall, Nashville, TN 37209
[3] Center of Excellence in Information Systems, Tennessee State University, 3500 John A. Merritt Blvd., Box 9501, Nashville, TN 37209
[4] The Observatories, Institute of Astronomy, Madingley Road, Cambridge, CB3 0HA United Kingdom
[5] Department of Physics and Astronomy, University of Victoria, BC V8W 3P6, Canada
[6] Division of Physics, Mathematics and Astronomy, 105-24, California Institute of Technology, Pasadena, CA 91125 USA
[7] Jet Propulsion Laboratory, California Institute of Technology, 4800 Oak Grove Dr., Pasadena, CA 91109 USA
[8] MIT Kavli Institute for Astrophysics and Space Research, MIT Department of Physics, 70 Vassar Street, Cambridge, MA 02139 USA
[9] Nicolaus Copernicus Astronomical Center, Polish Academy of Sciences, Rabianska 8, 87-100 Torun, Poland
[10] Guest worker, Dominion Astrophysical Observatory, Herzberg Institute of Astrophysics, National Research Council of Canada
[11] Visiting Astronomer, Kitt Peak National Observatory, National Optical Observatory, operated by the Association of Universities for Research in Astronomy, Inc., under cooperative agreement with the National Science Foundation.

determine fully the system parameters, including masses of the components at the sub-percent level.

Astrometry was obtained for the Palomar High-precision Astrometric Search for Exoplanet Systems (PHASES) program (Muterspaugh et al. 2006c), using the Palomar Testbed Interferometer (PTI) (Colavita et al. 1999), located on Palomar Mountain. That interferometer operated in the J (1.2 μ-m), H (1.6 μ-m), and K (2.2 μ-m) bands and combined starlight from two out of three available 40-cm apertures. The apertures formed a triangle with 86-, 87- and 110-m baselines.

2. OBSERVATIONS & MODELS

2.1. *PHASES Astrometry*

1 Gem was successfully observed with PTI on 29 nights in 2004–2007 with the phase-referenced fringe-scanning mode (Lane & Muterspaugh 2004) that was developed for high-precision astrometry. The data were reduced with the use of the algorithms described therein, together with the modifications described in Muterspaugh et al. (2005).

Our differential astrometry is listed in Muterspaugh et al. (2010a). Because PTI operated with a single baseline on a given night, the measurement errors are much smaller in the direction aligned with the baseline than they are in the orthogonal direction. To weight the data set properly when doing a combined fit with previous astrometry and radial-velocity data, we have fit an orbital model to the PHASES astrometry by itself. The resulting reduced χ^2 was 1.3, indicating a certain amount of excess scatter beyond the internal error estimates. We believe that this scatter is due to systematic noise sources that have been identified in the system (Muterspaugh et al. 2008). After re-scaling the uncertainties by a factor of $\sqrt{1.3}$ the median minor-axis formal uncertainty is 55 μseconds of arc, while the median major-axis uncertainty is 250 μseconds of arc. We also identify two points (MJD 54029.41661 and 54376.47755) as outliers, where the nightly data-reduction procedure misidentified the central fringe and calculated a separation that was in error by a factor of $\lambda/B \sim 4$ milliarcseconds (where λ is the operating wavelength and B is the interferometer baseline); those points were excluded from the subsequent fit.

2.2. *Previous Astrometry*

In addition to our astrometry, 1 Gem has been followed by a number of observers using speckle-interferometric techniques. We have incorporated 63 observations tabulated in the *4th Catalog of Interferometric Measurements of Binary Stars*[12] (Hartkopf et al. 2001) to constrain our fit further. Although of somewhat lower precision than our PHASES observations, the considerable time baseline (including observations between 1976 and 2005) of those additional measurements helps to constrain the parameters of the A–B visual binary. We fit the previous astrometry to a simple Keplerian model and rescale the uncertainties to yield $\chi^2_r = 1$. In many cases the published astrometry lacks uncertainties, so we derive uncertainties from the scatter of the data about a best-fit model. We find that uncertainties in separation should be increased by a factor of 1.95 and in position angle by a factor of 1.36. For the data points that lack uncertainties we assign a value of 3.96 mas in separation and 1.96 degrees in position angle.

[12] `http://ad.usno.navy.mil/wds/int4.html`

2.3. *Radial Velocity*

Extensive radial-velocity measurements of the 1 Gem system have been obtained in four separate campaigns spanning 40 years, including data from eight different instruments. We describe each data set below.

2.3.1. *Palomar, OHP & Cambridge Observations*

Between 1969 and 2009 R.F.G. acquired a total of 128 observations of 1 Gem using the radial-velocity spectrometer at Cambridge (Griffin 1967, 1980), a similar instrument at Palomar (Griffin & Gunn 1974; Griffin 1980), the CORAVEL spectrometer at Haute Provence Observatory (OHP; Baranne et al. 1979), and most recently, the Cambridge CORAVEL. The radial velocities obtained with the original Cambridge spectrometer and the Palomar spectrometer have been placed on the 'Cambridge' zero-point, which seems to be 0.8 km s^{-1} more positive than the zero-point favored by the Geneva group (Udry et al. 1999). Velocities acquired with the CORAVEL at Haute Provence have been shifted by +0.8 km s^{-1} from the values 'as reduced in Geneva', while the ones made since 1999 with the Cambridge CORAVEL have been adjusted by −0.1 from the 'as reduced' values. The preliminary relative weightings used for computing orbits were 0.1 for 'original Cambridge', 0.5 for Palomar and Haute Provence Observatory, and 1 for the Cambridge CORAVEL, except that recent observations (starting from the beginning of 2005) are so much better that they have been given weight 2. We have divided these data into two separate sets in order to allow for different velocity zeropoints: the Cambridge and Palomar data are referred to as data set A, while the OHP data are labeled set B. The data for components A and Ba are provided in Table 1.

2.3.2. *Dominion Astrophysical Observatory Observations and Reductions*

A series of observations of 1 Gem has been obtained by C.D.S. with the Dominion Astrophysical Observatory (DAO) radial-velocity spectrometer, in both its original (Fletcher et al. 1982) and subsequent (McClure et al. 1985) configurations. Observations were begun early in 1980 and continued until the end of 2003, shortly before the spectrometer was decommissioned. Masks based on the spectra of Arcturus and Procyon were found to give about equally good results, and all those available have been used at one time or another. Observations of IAU standard stars (Pearce 1957) have been used to adjust the observations made with each mask to the zero-point of Scarfe et al. (1990).

The DAO velocities of components A and Ba are listed in Table 2. It was not found necessary to apply corrections for blending, of the kind described by Scarfe et al. (1994), but a few velocities obtained from blended profiles have been rejected and omitted from that table, as have a few others whose residuals from a preliminary solution of the DAO velocities alone were over three times the root-mean-square value for the relevant star. The total number of acceptable velocities from DAO radial-velocity scanner observations is 123 of the primary star

and 107 of the brighter component of the close pair. The third component was not detectable in the DAO traces. We identify the DAO observations as data set C.

2.3.3. *KPNO Observations and Reductions*

From 1983 through 2009 F.C.F. obtained observations at the Kitt Peak National Observatory with the 0.9-m coudé feed telescope, coudé spectrograph, and several different CCD detectors. All of the spectrograms were acquired with a Texas Instruments (TI) CCD except for five that were obtained in 1983 with a RCA CCD and a single observation in 2008 September with a Tektronix CCD. All those observations were centered near 6430 Å and had typical signal-to-noise ratios of about 250. The numerous TI CCD spectra have a wavelength range of just 84 Å and a resolution of 0.21 Å . For additional information on the spectrograph and detector combinations see Fekel et al. (1988) and Fekel & Willmarth (2009).

Radial velocities from the 1983–1990 KPNO spectra were measured with the procedure described by Fekel et al. (1978). From 1991 onward the KPNO radial velocities were determined with the IRAF cross-correlation program FXCOR (Fitzpatrick 1993). The IAU radial-velocity standard stars of similar type to the components, HR 1283, β Gem, HR 3145, HR 4695 and 10 Tau, were used as reference stars for the correlations, and their radial velocities were adopted from the work of Scarfe et al. (1990).

Although we searched for lines of the third component in our red-wavelength TI CCD spectra by examining residual spectra that were made by removing the spectrum of component A, the late-type giant primary, we were not able to detect any evidence of the third star in our small wavelength window. While velocity measurement of component A, the late-type giant primary star, was straightforward, the FXCOR analysis of the component Ba, the F-type star, requires some explanation. The strongest lines of the F star are very weak in the 6430 Å region, and most are usually very blended with lines of the late-type giant primary. Given the limited wavelength range for nearly all of the KPNO spectrograms, cross-correlation of the entire region produces spurious velocities of the F star because of the line blending. So instead, the radial velocities of Ba were obtained by cross-correlating the regions around just one or two of its least-blended lines in each spectrum. The 86 velocities of component A and 80 of component Ba are listed in Table 3. They are identified as data set D.

2.3.4. *Tennessee State University Observations and Reductions*

From 2004 January through 2008 April J.A.E. acquired 522 spectrograms with the Tennessee State University 2-m Automatic Spectroscopic Telescope (AST), fiber-fed echelle spectrograph, and a 2048 x 4096 SITe ST-002A CCD. The echelle spectrograms have 21 orders, covering the wavelength range 4920–7100 Å with an average resolution of 0.17 Å. The typical signal-to-noise ratio is ∼50. Eaton & Williamson (2004) have given a more extensive description of the telescope, situated at Fairborn Observatory near Washington Camp in the Patagonia Mountains of southeastern Arizona.

Velocities of two components, A and Ba, were determined by fitting Gaussians to the lines of the two stars in succession in a cross-correlation function calculated for a list of solar Fe I lines, all treated as delta functions of equal weight (Eaton & Williamson 2007). Those AST spectra are referred to as data set E. After the measurements of components A and Ba were completed, M.H.W. re-examined the AST spectra. He found that by subtracting a model of the primary stellar spectrum, obtained by averaging over all available spectra (appropriately shifted), a barely detectable feature corresponding to the Bb component could be seen and measured. Fekel et al. (2009) described the general velocity reduction procedure that was used for those measurements, but which previously did not include the subtraction step. We note here that that reduction method used a line list similar to that for the A and Ba components. Figure 1 shows sample spectra both before and after subtraction. The lower curve is the average of nearly 170 moderately strong lines plotted atop each other in the velocity space around component A. The upper curve shows the same velocity range with the average primary spectrum subtracted. Owing to the extreme weakness of the component Bb lines, only a minority of our AST spectra were amenable to this technique. Nevertheless, results are included in Table 4 for the 99 spectra that yielded usable velocities for the Bb component.

It was noted in the reduction of data set E that some of the lines of the close binary are sufficiently blended with the dominant K-giant's lines that systematic errors could potentially be introduced. We checked this possibility by fitting a model that is limited to only those points in data set E where velocities for all three components are available. The resulting parameters were not significantly different from the fit to all of the data. However, the χ^2_r of the fit was decreased and the residual velocity scatter was smaller. On the basis of the ratio of residuals we therefore assign separate weights to the two types of data. Points where only the A and Ba components yielded velocities were assigned 25% larger uncertainties than the points when all three were visible.

2.4. *Orbital Models*

In modeling the hierarchical triple system we make the simplifying assumption that the two orbital systems do not perturb each other, i.e., we use a pair of Keplerian orbital systems, one wide (A–B) and slow (13.3-year period), the other a close (Ba–Bb) 9.6-day system. Note that one cannot simply superimpose the separation vectors from the two models; this is because the PHASES observable is the angle between the two Centers-of-Light (COL) of the system. Since the A component is single its center of mass (CM) coincides with its COL. However, for the Ba–Bb system a CM–COL coupling amplitude of the form

$$\overrightarrow{y_{\rm obs}} = \overrightarrow{r_{\rm A-B}} - \frac{R-L}{(1+R)\,(1+L)}\overrightarrow{r_{\rm Ba-Bb}} \qquad (1)$$

is required. Here $R = M_{\rm Bb}/M_{\rm Ba}$ is the close-orbit mass ratio and $L = L_{\rm Bb}/L_{\rm Ba}$ the luminosity ratio. Including this coupling term for astrometric data is important when a full analysis including radial-velocity data is made. It should be noted that this coupling equation is an approximation valid when $r_{\rm Ba-Bb} \ll \lambda/B$ and/or $\rm L \ll 1$.

TABLE 1
1 Gem Radial Velocity Data Sets A & B (Palomar, OHP & Cambridge)

HJD−2400000.5	Velocity (A) ($km\,s^{-1}$)	σ	O−C	Velocity (Ba) ($km\,s^{-1}$)	σ	O−C	Code
40335.84	39.1	0.79	−0.19	···	···	···	213
40492.22	35.6	0.79	0.11	···	···	···	213
40494.22	33.9	0.79	−1.54	···	···	···	213
40577.92	33.0	0.79	−0.22	···	···	···	213
40592.90	32.8	0.79	−0.03	···	···	···	213
40986.90	22.8	0.79	−1.99	···	···	···	213
41285.04	20.8	0.79	−0.76	···	···	···	213
41290.10	23.0	0.79	1.47	···	···	···	213
41639.12	19.5	0.79	−0.17	···	···	···	213
41652.08	18.0	0.79	−1.63	···	···	···	213

Note. — Radial-Velocity data for the 1 Gem system from CORAVEL observations, the uncertainties and the fit residuals (O−C values) for the fit. The numbers in the code column of the data set for the respective sources are 213 for 'old Cambridge', 218 for Palomar, 313 for the CORAVEL at Haute Provence, and 312 and (post-2005) 412 for Cambridge CORAVEL. The data shown are a stub; the full data set is available in the online version.

TABLE 2
1 Gem Radial Velocity Data Set C (DAO)

HJD−2400000.5	Velocity (A) ($km\,s^{-1}$)	σ	O−C	Velocity (Ba) ($km\,s^{-1}$)	σ	O−C
44257.279	30.1	0.66	0.01	···	···	···
44291.217	31.2	0.66	0.61	74.2	1.40	1.05
44298.200	31.4	0.66	0.71	···	···	···
44304.230	31.3	0.66	0.52	−7.0	1.40	0.16
44321.240	30.7	0.66	−0.34	61.8	1.40	1.65
44339.146	31.0	0.66	−0.32	70.4	1.40	−2.05
44492.548	33.4	0.66	−0.45	68.9	1.40	−0.96
44548.415	34.1	0.66	−0.72	···	···	···
44614.297	36.4	0.66	0.41	−11.6	1.40	0.31
44670.137	37.2	0.66	0.23	−34.5	1.40	−0.16

Note. — Radial-Velocity data for the 1 Gem system from DAO , together with the uncertainties and the fit residuals (O−C values) for the fit. The data shown are a stub; the full data set is available in the online version.

TABLE 3
1 Gem Radial Velocity Data Set D (KPNO)

HJD−2400000.5	Velocity (A) ($km\,s^{-1}$)	σ	O−C	Velocity (Ba) ($km\,s^{-1}$)	σ	O−C
45358.292	34.6	0.67	0.08	···	···	···
45360.278	34.0	0.67	−0.47	···	···	···
45361.141	34.9	0.67	0.45	−29.5	1.35	3.71
45447.131	32.0	0.67	−0.17	−28.2	1.35	0.22
45451.156	32.5	0.67	0.44	···	···	···
45596.486	28.1	0.67	−0.37	72.9	1.35	−1.65
45719.366	26.4	0.67	0.48	···	···	···
45720.305	26.5	0.67	0.60	67.5	1.35	−0.28
45721.249	26.4	0.67	0.52	74.4	1.35	−1.98
45811.111	24.2	0.67	−0.13	−10.1	1.35	−0.38

Note. — Radial-Velocity data for the 1 Gem system from KPNO, together with the uncertainties and the fit residuals (O−C values) for the fit. The data shown are a stub; the full data set is available in the online version.

TABLE 4
1 Gem Radial Velocity Data Set E (AST)

HJD−2400000.5	Velocity (A) ($km\,s^{-1}$)	σ	O−C	Velocity (Ba) ($km\,s^{-1}$)	σ	O−C	Velocity (Bb) ($km\,s^{-1}$)	σ	O−C
52895.5211	20.3	0.09	0.02	−15.3	0.36	−0.18	103.1	2.00	0.22
52897.5268	20.3	0.11	0.01	44.2	0.45	−0.38	···	···	···
52898.4772	20.3	0.09	0.00	70.2	0.36	−0.16	−45.0	2.00	−3.64
52899.4790	20.2	0.09	−0.10	81.2	0.36	0.58	−56.7	2.00	1.98
52903.4876	20.4	0.09	0.08	−16.4	0.36	0.47	106.0	2.00	0.24
52904.4837	20.3	0.09	−0.03	−22.3	0.36	0.42	118.0	2.00	2.37
52908.4779	20.3	0.09	−0.05	77.0	0.36	0.04	−52.0	2.00	0.58
52909.4750	20.3	0.09	−0.05	79.0	0.36	0.34	−55.0	2.00	0.46
52910.4751	20.4	0.11	0.04	59.6	0.45	−0.24	···	···	···
52912.4727	20.4	0.09	0.04	−2.6	0.36	0.85	88.5	2.00	5.46

Note. — Radial-Velocity data for the 1 Gem system from AST, together with the uncertainties and the fit residuals (O−C values) for the fit. The data shown are a stub; the full data set is available in the online version.

To combine optimally the large number of different data sets, taken by different instruments, we group the available radial-velocity data into 5 separate sets (labeled A through E) and solve for a separate zero-point offset for each data set.

3. RESULTS

The best-fit orbital model was found with the use of an iterative non-linear least-squares-minimization scheme. The best-fit parameters are given in Table 5. The combined fit to PHASES, radial-velocity, and previous differential astrometry has 1989 data points with 22 free parameters. The reduced χ^2_r of the fit is 1.16.

A fit to the the inner orbit (Bab) with the inner eccentricity as a free parameter results in a slightly non-zero value ($e_{Bab} = 0.0024 \pm 0.0005$). Bassett's test (Bassett 1978) yields a T_1 statistic ($\sim$20), indicating that the eccentricity of the orbit is significant. However, we noticed that separate fits to the individual radial velocity data sets yields slightly inconsistent results (ranging from 0.003 to 0.01), with inconsistent values for ω. We therefore report the results for three fits in Table 5; one fit including all data sets and the eccentricity fixed to 0, a second fit including all data and the eccentricity a free parameter, and a third fit to only the A,B,C & D data sets. We find that all three fits are consistent to within the uncertainties, and the variable-eccentricity fit to all of the data yields the smallest uncertainties. We therefore use the results from the variable-eccentricity fit to all data to derive the system parameters shown in Table 6, for the figures, and for the O–C residuals in the data tables. The estimated component masses for all three fitrs change by less than 1σ.

It should be noted that even with both COL-astrometry and radial-velocity data, there exists a parameter degeneracy corresponding to an exchange of the ascending and descending nodes together with a change in the luminosity ratio of the short-period subsystem (interchanging which is the brighter star). Given one solution for the mass and luminosity ratios ($\frac{m_1}{m_2}$ and $\frac{l_1}{l_2}$), the other possible luminosity ratio can be found from

$$L_2 = \frac{2\frac{m_1}{m_2} + \frac{m_1}{m_2}\frac{l_1}{l_2} - \frac{l_1}{l_2}}{1 + 2\frac{l_1}{l_2} - \frac{m_1}{m_2}} \quad (2)$$

However, given the values we find ($\frac{l_1}{l_2} \sim 0$ and $\frac{m_1}{m_2} = 0.59$) the corresponding alternate luminosity ratio is not physically plausible ($L_2 = 2.9$).

The best-fit value of the K–band luminosity ratio L_{Bb}/L_{Ba} is not significantly different from zero; as a result we are not able to place more than a limit on the absolute magnitude of the Bb component.

3.1. *Relative Orbital Inclinations*

The mutual inclination Φ of two orbits is given by

$$\cos\Phi = \cos i_{AB}\cos i_{Bab} + \sin i_{AB}\sin i_{Bab}\cos\left(\Omega_{AB} - \Omega_{Bab}\right) \quad (3)$$

where i_{AB} and i_{Bab} are the orbital inclinations and Ω_{AB} and Ω_{Bab} are the longitudes of the ascending nodes.

The mutual inclination of the orbits in the 1 Gem system is 136.2 ± 1.6 degrees (Table 6); it is within the range where Kozai cycles occur (39°.2–140°.8; Kozai (1962)), albeit close to a limit. Fabrycky & Tremaine (2007) predicted an increased frequency of systems with mutual inclinations near the limits. This result is consistent with predicted outcomes of Kozai Cycle + Tidal Friction (KCTF) evolution (viz. large period ratio, near-circular inner binary, near-critical mutual inclination).

3.2. *Component Masses and Distance*

In Table 6 various derived parameters, including the individual masses, are listed. These parameters are based on the results from the fit with non-zero eccentricity. From our orbital analysis the distance to the 1 Gem system is found to be 46.76 ± 0.07 pc; that compares well to the revised *Hipparcos* value of 46.9 ± 2.0 (van Leeuwen 2007).

Because of its faint magnitude, the spectral type of Bb can not be estimated from even our summed spectra. The only estimate that can be given is by comparing its mass to canonical values of spectral type vs mass relations. On the assumption that component Bb is a main sequence star and not a white dwarf, its mass of 1.012 $M_\odot$ (Table 6) corresponds to a G2V star (Cox 1999).

3.3. *Component Luminosities*

As part of the combined astrometric and radial-velocity fit we can solve for the K-band luminosity ratios of the components. This is because the distance and subsystem total mass are essentially determined by the observations of the wide A–B system, while the sub-system mass ratio is found from the sub-system radial velocities. Therefore, this leaves only the component luminosity ratios dependent on the size of the observed astrometric perturbation.

The PTI cannot provide precise determinations of the total system magnitude m_K nor the A–B system differential magnitude Δm_K. Instead, a Keck adaptive optics image of 1 Gem was obtained on MJD 53,227 with a narrow-band H_2 2-1filter centered at 2.262 μm. We measured the A–B differential magnitude to be $\Delta m_{H2} = 2.043 \pm 0.008$. Neugebauer & Leighton (1969) list the K-band magnitude of the 1 Gem system as 2.21 ± 0.06. Using those photometric measurements, together with the parallax and upper limit to the Ba–Bb intensity ratio determined here, we derive the resulting absolute K magnitudes and list them in Table 6.

4. CONCLUSIONS

PHASES interferometric astrometry has been used together with very extensive radial-velocity data to measure the orbital parameters of the triple-star system 1 Geminorum, and in particular to resolve the apparent orbital motion of the close Ba-Bb pair. The amplitude of the Ba-Bb COL motion is only 970 ± 60 μarcseconds, indicating the level of astrometric precision attainable with interferometric astrometry. The orbital period of the outer A–B pair is 13.354 ± 0.002 yrs, while that of the inner Ba–Bb pair is 9.596558 ± 0.000004 days.

By using astrometry and radial velocities to measure both orbits, we are able to determine the mutual inclination of the orbits, which we find to be $136°.2 \pm 1°.6$. Such a mutual inclination implies Kozai oscillations unless damped by other interactions.

We also present the first direct detection of the tertiary component, Bb, in this system. The combination

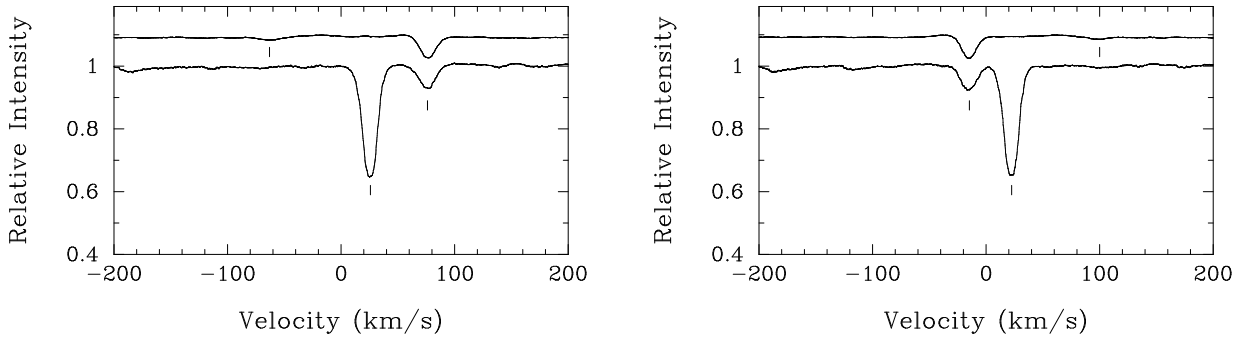

FIG. 1.— (Left) From an AST spectrum of the 1 Gem system, the lower solid line is the average profile of the components, summed from about 170 spectral regions. Tick marks indicate the positions of the Ba (F-subgiant) and A (K-giant) components. The upper line, arbitrarily vertically shifted for visibility, is the remainder after a model of the K-giant component has been removed from the lower line. The position of the extremely weak third component, Bb, is indicated. (Right) The same results for another AST spectrum at an orbital phase with the Ba and Bb components reversed.

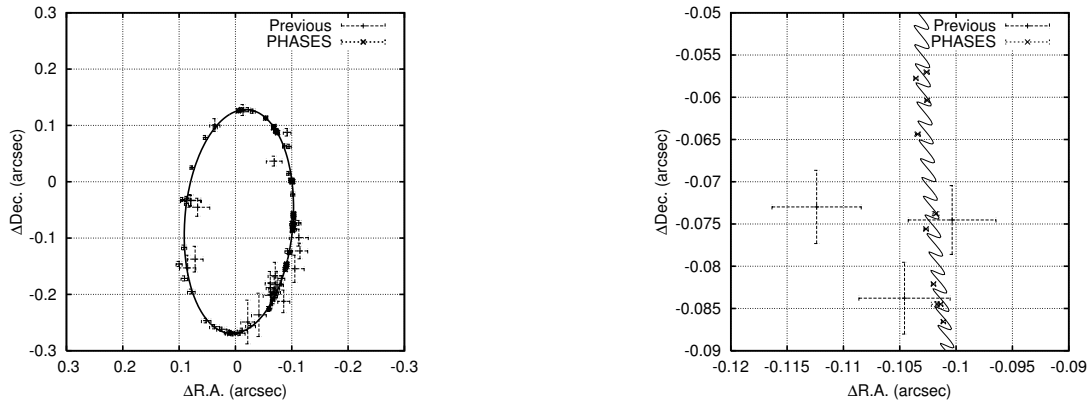

FIG. 2.— (left) The best-fit visual orbit of the 1 Gem A–Bab system, together with previously available astrometric data and our PHASES astrometry. We note that the error ellipses of the PHASES data appear smaller than the points used to indicate the data. (right) A close-in view of a sub-section of the PHASES astrometry, together with the best-fit orbital model.

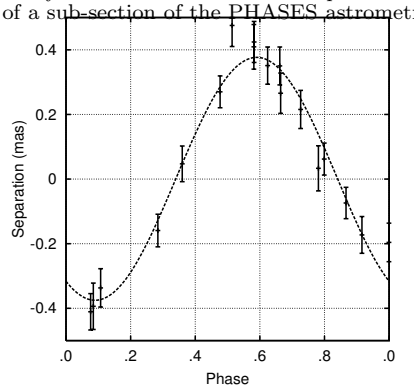

FIG. 3.— The astrometric orbit of the 1 Gem Bab sub-system projected along an axis rotated 155 degrees East of North. The motion in the A–B system has been removed. The axis corresponds to the most common orientation of the minor axis of the positional error ellipses (which vary slightly from night to night, and between baselines). For clarity, only those observations where the projected uncertainty is less than 300 μs of arc have been included in the plot (all observations are included in the fit).

of radial-velocity data for all three components and high-precision astrometry allows us to constrain the mass ratio of the B subsystem as well as solve for the complete set of system parameters. Finally we have been able to determine the component masses with precision in the 0.5% range, and the distance to the system to 0.15%, among the most precise mass and distance determinations available for stellar multiple systems.

We wish to acknowledge the extraordinary observational efforts of K. Rykoski. Observations with PTI were made possible thanks to the efforts of the PTI Collaboration, which we acknowledge. We also thank the Dominion Astrophysical, Palomar, and Geneva observatories for allowing RFG to obtain radial velocities of 1 Gem. We also thank Lou Boyd, Director of Fairborn Observatory, for dedication to robotic astronomy and excellent maintenance of a unique observatory. This research has made use of services from the Michelson Science Center, California Institute of Technology, http://msc.caltech.edu. Part of the work described in this paper was performed at the Jet Propulsion Laboratory under contract with the National Aeronautics and Space Administration. This research has made use of the Simbad database, operated at CDS, Strasbourg, France, and of data products from the Two-Micron All-Sky Survey, which is a joint project of the University of Massachusetts and the Infrared Processing and Analysis Center/California Institute of Technology, funded by the NASA and the NSF. MWM acknowledges support from State of Tennessee's Centers of Excellence Program, and the Townes Postdoctoral Fellowship Program.

REFERENCES

Abt, H. A., Kallarakal, V. V., 1963, ApJ, 138, 140.

Baranne, A., Mayor, M., & Poncet, J. L. 1979, Vistas in Astron., 23, 279

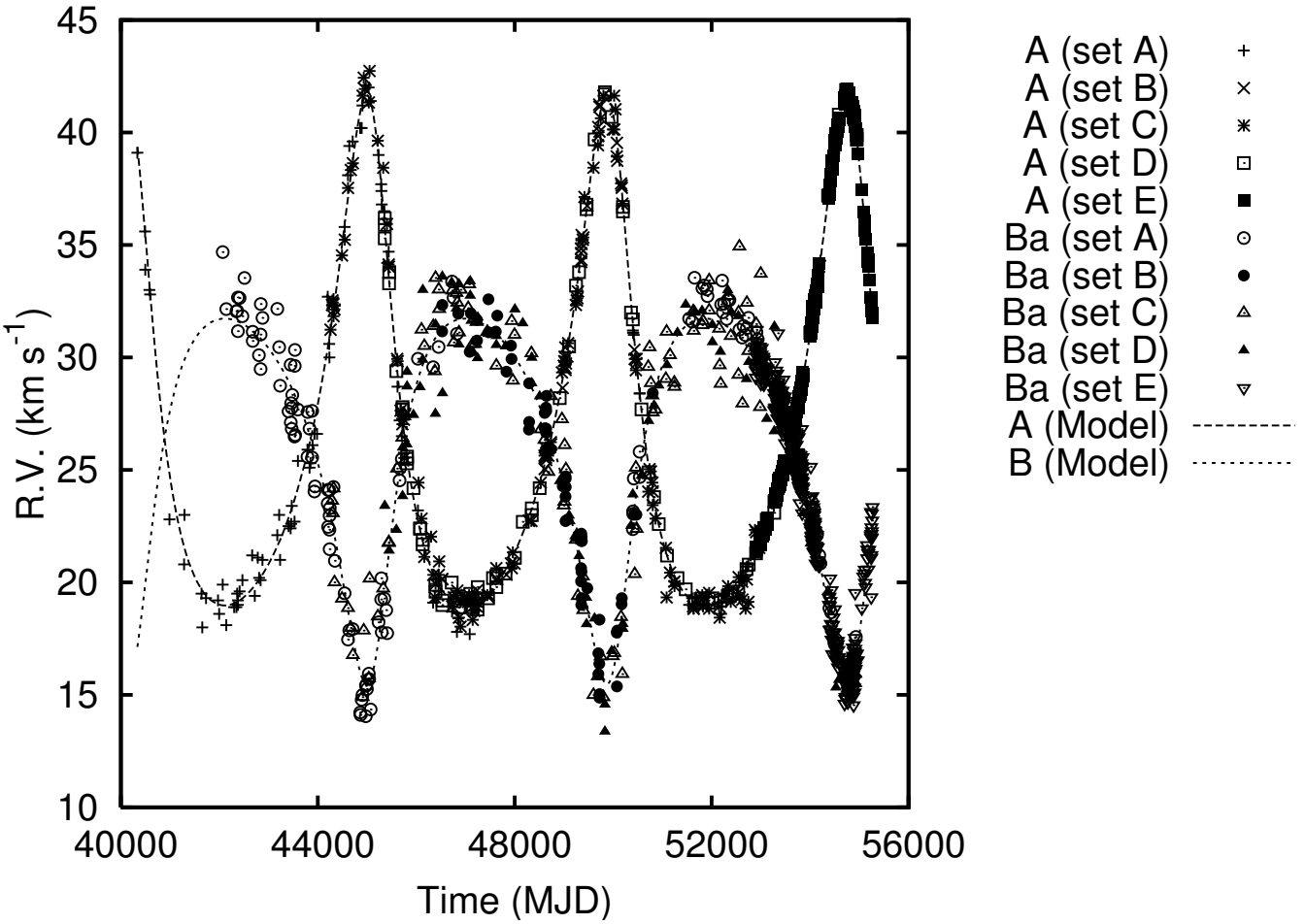

FIG. 4.— Radial velocities of 1 Gem compared with the computed orbit of the A–B system as a function of time. The motion due to the Ba–Bb orbit has been removed.

Bassett, E. E. 1978, The Observatory, 98, 122
Boden, A., Creech-Eakman, M., Queloz, D., 2000, ApJ, 536, 880-890.
Colavita, M. M., et al. 1999, ApJ, 510 , 505.
Colavita, M. M., 1999, PASP, 111, 111.
Colavita, M., et al. 2003, ApJ, 592, L83
Cox, A. N., 1999, Allen's Astrophysical Quantities, Springer-Verlag, New York.
Eaton, J. A., & Williamson, M. H. 2004, Proc. SPIE, 5496, 710
Eaton, J. A., & Williamson, M. H. 2007, PASP, 119, 886
Eggleton, P. P., & Tokovinin, A. A. 2008, MNRAS, 389, 869
Fabrycky, D., & Tremaine, S. 2007, ApJ, 669, 1298
Fekel, F., Bopp, B. W., & Lacy, C. H. 1978, AJ, 83, 1445
Fekel, F. C., Gillies, K., Africano, J., & Quigley, R. 1988, AJ, 96, 1426
Fekel, F. C., Joyce, R. R., Hinkle, K. H., & Skrutskie, M. F. 2000, AJ, 119, 1375
Fekel, F. C., Tomkin, J., & Williamson, M. H. 2009, AJ, 137, 3900
Fekel, F. C., & Willmarth, D. W. 2009, PASP, 121, 1359
Fitzpatrick, M. J. 1993, in ASP Conf. Ser. 52, Astronomical Data Analysis Software and Systems II, ed. R. J. Hanish, R. V. J. Brissenden, & J. Barnes (San Francisco: ASP), 472
Fletcher, J.M., Harris, H.C., McClure, R.D., & Scarfe, C.D. 1982, PASP, 94, 1017
Griffin, R. F. 1967, ApJ, 148, 465
Griffin, R. F. 1980, Sky & Telescope, 59, 19
Griffin, R. F., & Gunn, J. E. 1974, ApJ, 191, 545
Griffin, R. F., & Radford, G. A. 1976, The Observatory, 96, 188
Hartkopf, W. I., McAlister, H. A., & Mason, B. D. 2001, AJ, 122, 3480
Kiseleva, L. G., Eggleton, P. P., & Mikkola, S. 1998, MNRAS, 300, 292
Kiseleva-Eggleton, L., & Eggleton, P. P. 2001, Evolution of Binary and Multiple Star Systems, Astronomical Society of the Pacific Conference Series, Vol. 229, 91
Kozai, Y. 1962, AJ, 67, 591
Kuiper, G. P. 1948, ApJ, 108, 542
Lane, B. F., & Muterspaugh, M. W. 2004, ApJ, 601, 1129
Lane, B. F., et al. 2007, ApJ, 669, 1209
Lestrade, J.-F., Phillips, R. B., Hodges, M. W., & Preston, R. A. 1993, ApJ, 410, 808
Massarotti, A., Latham, D. W., Stefanik, R. P., & Fogel, J. 2008, AJ, 135, 209
Mazeh, T., & Shaham, J. 1979, A&A, 77, 145
McClure, R.D., Fletcher, J.M., Grundmann, W.A. & Richardson, E.H. 1985, in Stellar Radial Velocities, ed. A.G.D. Philip and D.W. Latham, (L. Davis Press, Schenectady), p. 49
Muterspaugh, M. W., Lane, B. F., Konacki, M., Burke, B. F., Colavita, M. M., Kulkarni, S. R., & Shao, M. 2005, AJ, 130, 2866
Muterspaugh, M. W., Lane, B. F., Konacki, M., Burke, B. F., Colavita, M. M., Kulkarni, S. R., & Shao, M. 2006, A&A, 446, 723
Muterspaugh, M. W., Lane, B. F., Konacki, M., Wiktorowicz, S., Burke, B. F., Colavita, M. M., Kulkarni, S. R., & Shao, M. 2006, ApJ, 636, 1020
Muterspaugh, M. W., Lane, B. F., Kulkarni, S. R., Burke, B. F., Colavita, M. M., & Shao, M. 2006, ApJ, 653, 1469
Muterspaugh, M. W., et al. 2008, AJ, 135, 766
Muterspaugh, M. W., Lane, B. F., Kulkarni, S. R., et al. 2010, AJ, 140, 1579

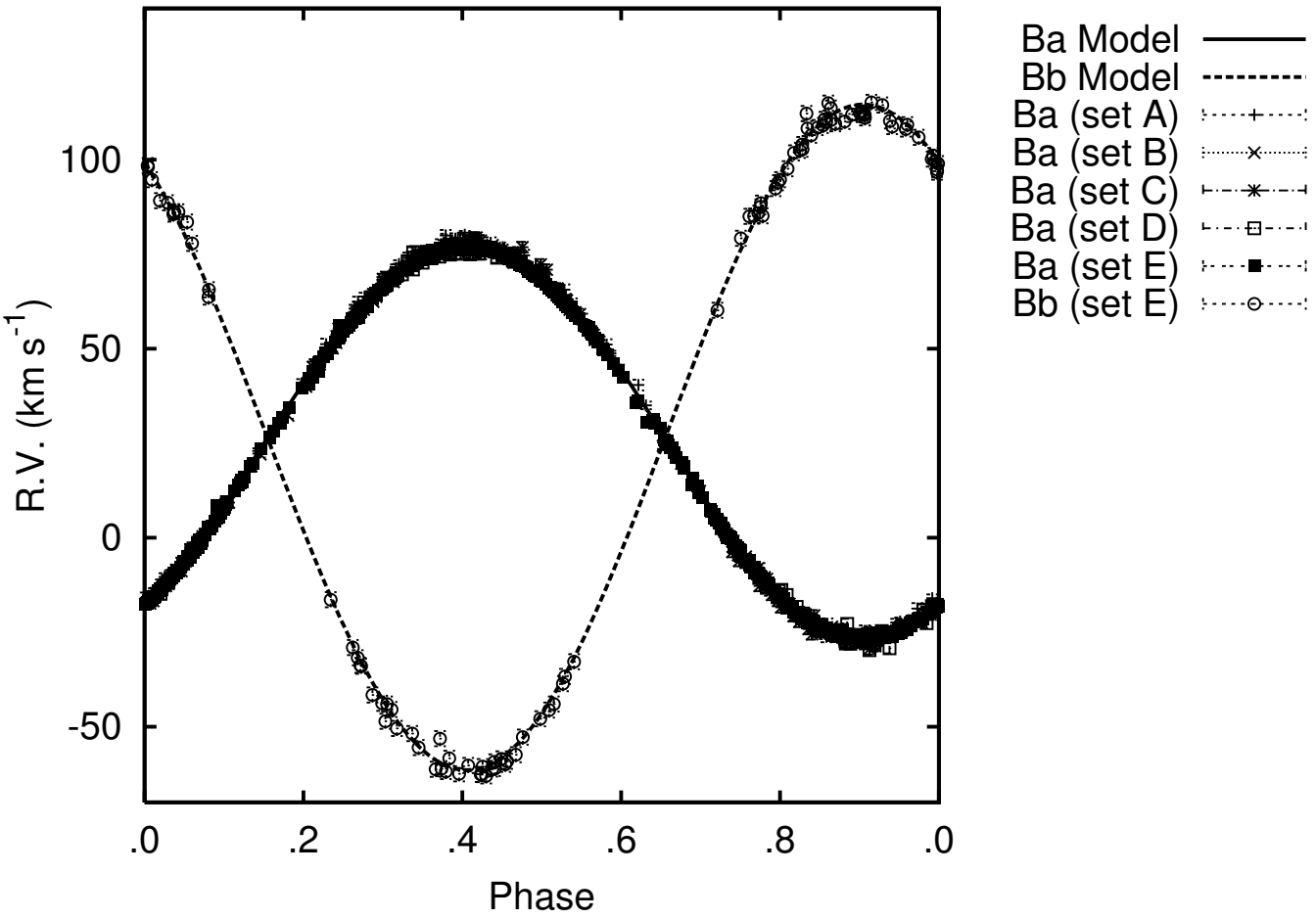

FIG. 5.— Radial velocities of 1 Gem Ba and Bb compared with the computed orbit. Motion in the A–B system has been removed.

Muterspaugh, M. W., et al. 2010, AJ, 140, 1646
Neugebauer, G., & Leighton, R. B. 1969, NASA SP, Washington: NASA, 1969,
Pearce, J.A. 1957, Trans. IAU, 9, 441
Scarfe, C.D., Barlow, D.J., Fekel, F.C., Rees, R.F., Lyons, R.W., Bolton, C.T., McAlister, H.A., & Hartkopf, W.I. 1994, AJ, 107, 1529
Scarfe, C. D., Batten, A. H., & Fletcher, J. M. 1990, Publ. Dom. Astrophys. Obs., 18, 21
Skrutskie, M. F. et al, 2006, AJ, 131, 1163.
Strassmeier, K. G., & Fekel, F. C. 1990, A&A, 230, 389
Sterzik, M. F., & Tokovinin, A. A. 2002, A&A, 384, 1030
Söderhjelm, S. 1999, A&A, 341, 121
Tokovinin, A. A. 1997, A&AS, 124, 75
Tokovinin, A. 2008, MNRAS, 389, 925
Tokovinin, A., Thomas, S., Sterzik, M., & Udry, S. 2006, A&A, 450, 681
Torres, G., & Ribas, I. 2002, ApJ, 567, 1140
Udry, S., Mayor, M., & Queloz, D. 1999, in ASP Conf. Ser. 185, Precise Stellar Radial Velocities, ed. J. B. Hearnshaw & C. D. Scarfe (San Francisco: ASP), 367
van Leeuwen, F. 2007, *Hipparcos*, The New Reduction of the Raw Data, Astrophysics and Space Sciences Library, Vol. 350, (Dordrecht: Springer)

TABLE 5
Best-fit Orbital Parameters for 1 Gem

Parameter	Floating e Value	Uncertainty	Fixed e Value	Uncertainty	Data Sets ABCD Only Value	Uncertainty	Previous Value
χ^2	2390.90		2414.43		933.70		
χ_r	1.16		1.17		1.02		
P_{AB}(days)	4877.6	±1.0	4877.6	±1.0	4877.7	±1.0	4821.3 [a]
e_{AB}	0.3709	±0.0004	0.3711	±0.0004	0.3712	±0.0005	0.34 [a]
i_{AB}(deg.)	59.33	±0.04	59.34	±0.04	59.34	±0.05	62 [a]
ω_{AB}(deg.)	21.29	±0.09	21.32	±0.09	21.3	±0.1	190 [a]
T_{AB}(MJD)	45118.5	±2.3	45118.7	±2.3	45118.5	±2.3	
Ω_{AB}(deg.)	353.67	±0.04	353.67	±0.04	353.65	±0.04	178 [a]
$M_A(M_\odot)$	1.94	±0.01	1.94	±0.01	1.97	±0.03	
$M_B(M_\odot)$	2.719	±0.008	2.722	±0.008	2.73	±0.02	
d(pc)	46.76	±0.07	46.77	±0.08	46.9	±0.2	
P_{Bab}(days)	9.596558	±0.000004	9.596558	±0.000004	9.596547	±0.000006	9.59659 ± 0.00004 [b]
e_{Bab}	0.0024	±0.0005	0.0	···	0.005	±0.001	0.0 [b]
i_{Bab}(deg.)	93.2	±1.1	93.2	±1.1	95.1	±1.3	
ω_{Bab}(deg.)	164.3	±11.8	···	···	55.1	±14.7	
$T_{0,Bab}$(MJD)	53220.5	±0.3	···	···	···	···	··· [b]
$T_{0,Bab}$(MJD)[c]	···	···	53216.1267	±0.0009	53217.6	±0.4	40443.129 ± 0.015 [b]
Ω_{Bab}(deg.)	137.5	±1.9	137.5	±1.9	137.5	±1.8	
M_{Bb}/M_{Ba}	0.593	±0.001	0.592	±0.001	0.599	±0.004	
L_{Bb}/L_{Ba}(K-band)	0.00	±0.02	0.00	±0.02	0.01	±0.02	
V_0(A, km/s)	26.38	±0.03	26.38	±0.03	26.38	±0.03	
V_0(B, km/s)	25.4	±0.1	25.4	±0.1	25.4	±0.1	
V_0(C, km/s)	25.28	±0.06	25.27	±0.06	25.26	±0.06	
V_0(D, km/s)	25.11	±0.04	25.11	±0.04	25.11	±0.04	
V_0(E, km/s)	25.254	±0.007	25.250	±0.007	···	···	
No.Param.	22		20		22		
No.Pts.	1989		1989		846		
σ_A (km/s)	A: 0.65	Ba: 1.04	A: 0.65	Ba: 1.04	A: 0.65	Ba: 0.92	
σ_B (km/s)	A: 0.35	Ba: 0.89	A: 0.35	Ba: 0.88	A: 0.35	Ba: 0.96	
σ_C (km/s)	A: 0.66	Ba: 1.42	A: 0.66	Ba: 1.43	A: 0.66	Ba: 1.29	
σ_D (km/s)	A: 0.30	Ba: 1.33	A: 0.30	Ba: 1.33	A: 0.30	Ba: 1.46	
σ_E (km/s)	A: 0.11	Ba: 0.50 Bb: 2.07	A: 0.11	Ba: 0.52 Bb: 2.05	···	···	

[a] From Söderhjelm (1999)
[b] From Griffin & Radford (1976)
[c] Time of maximum R.V.

TABLE 6
Derived System Parameters for 1 Gem

Parameter	Value & Uncertainty
Φ_{AB-Bab} (deg)	136.2 ± 1.6
π (arcsec)	0.02139 ± 0.00003
a_{AB} (arcsec)	0.2010 ± 0.0004
a_{Bab} (arcsec)	0.002638 ± 0.000005
$a_{Bab,C.O.L}$ (arcsec)	0.00097 ± 0.00006
a_{AB} (A.U.)	9.399 ± 0.010
a_{Bab} (A.U.)	0.1234 ± 0.0001
K_A ($km\,s^{-1}$)	11.34 ± 0.03
K_B ($km\,s^{-1}$)	8.07 ± 0.04
K_Ba ($km\,s^{-1}$)	52.0 ± 0.1
K_Bb ($km\,s^{-1}$)	87.7 ± 0.2
m_A ($M_\odot$)	1.94 ± 0.01
m_{Ba} ($M_\odot$)	1.707 ± 0.005
m_{Bb} ($M_\odot$)	1.012 ± 0.003
$M_{K,A}$ (mag)	-0.99 ± 0.06
$M_{K,Ba}$ (mag)	1.06 ± 0.07